WORLDVIEW-2 PAN-SHARPENING

Chris Padwick[1], Principal Scientist
Michael Deskevich[2], Sr. Software Engineer
Fabio Pacifici[1], Principal Scientist
Scott Smallwood[1], Sr. Software Engineer
[1] DigitalGlobe, 1601 Dry Creek Drive, Suite 260, Longmont CO, 80503, USA
[2] ITT Visual Information Solutions, 4990 Pearl East Circle, Boulder CO, 80301, USA
cpadwick@digitalglobe.com
mdeskevich@ittvis.com
fpacific@digitalglobe.com

ABSTRACT

A novel pan-sharpening algorithm designed for sharpening WorldView-2 (WV-2) imagery is presented. The WV-2 satellite was launched by DigitalGlobe on Oct 8 2009. WV-2 has 8 spectral bands covering the range from 400nm-1050nm and a panchromatic band covering 450nm-800nm. The proposed pan-sharpening algorithm accepts any number of input bands, and quantitative color comparisons are performed using different band combinations from original multi-spectral file. The pan-sharpening algorithm is found to produce acceptable color recovery and spatial recovery for a wide variety of input scenes.

INTRODUCTION

The WorldView-2 (WV-2) satellite, launched by DigitalGlobe on Oct 8 2009 represents the first commercial imaging satellite to collect very high spatial resolution data in 8 spectral bands. The multi-spectral bands cover the spectral range from 400nm-1050nm at a spatial resolution of 1.84m, while the panchromatic band covers the spectrum from 450nm-800nm with 4x greater spatial resolution, 0.46m. The relative spectral responses from each band are shown in Figure 1.

It is often desired to have the high spatial resolution and the high spectral resolution information combined in the same file. Pan-sharpening is a type of data fusion that refers to the process of combining the lower-resolution color pixels with the higher resolution panchromatic pixels to produce a high resolution color image.

Many pan-sharpening techniques exist in the literature [Nikolakopoulos 2008]. One common class of algorithms for pan-sharpening is called "component substitution," where one generally performs the following steps:

- **Up-sampling**: the multispectral pixels are up-sampled to the same resolution as the panchromatic band;
- **Alignment**: the up-sampled multispectral pixels and the panchromatic pixels are aligned to reduce artifacts due to mis-registration (generally, when the data comes from the same sensor, this step is usually not necessary);
- **Forward Transform**: the up-sampled multispectral pixels are transformed from the original values to a new representation, which is usually a new color space where intensity is orthogonal to the color information;
- **Intensity Matching**: the multi-spectral intensity is matched to the panchromatic intensity in the transformed space;
- **Component Substitution**: the panchromatic intensity is then directly substituted for the multi-spectral intensity component;
- **Reverse Transform**: the reverse transformation is performed using the substituted intensity component to transform back to the original color space.

If the above transformation is perfect, then the resulting imagery will have the same sharpness as the original panchromatic image as well as the same colors as the original multispectral image. In practice, however, it is often impossible to meet both of these goals and one often trades sharpness for color recovery or vice-versa.

A significant factor that affects the color recovery in the resulting image is how well the forward transformation models the relationship between the panchromatic and multispectral bands.

[1] DigitalGlobe, 1601 Dry Creek Drive, Suite 260, Longmont CO, 80503, USA
[2] ITT Visual Information Solutions, 4990 Pearl East Circle, Boulder CO, 80301, USA

A very simple algorithm for pan-sharpening is called the Hue-Intensity-Saturation (HIS) sharpening algorithm, which utilizes the well known HIS color space. The conversion from the RGB color space to HIS color space is well known (Tu 2004) and is not repeated here. The HIS color space has the advantage that the three components are independent, thus manipulating one component cannot affect the other components. In the HIS color space, the intensity component ("I") is a simple average of the three color components:

$$I = \tfrac{1}{3}\left(R + G + B\right) \qquad \textbf{Equation 1}$$

where R indicates the pixel value for the red band, G indicates the pixel value for the green band, and B indicates the pixel value for the blue band. However, it is noted (Tu 2001) that the multi-spectral intensity as represented above is a poor match for the panchromatic band, even after intensity matching is applied.

In most cases, the panchromatic intensity is not modeled well by this equation, and the resulting color distortion makes the resulting product undesirable. There are two main reasons why the HIS method does not work well for these images:

- The HSI model presumes a single device dependent wavelength for each of R, G and B when defining the transformation RGB to HSI, while the imagery is taken with sensors responding to band of wavelengths in each of the R, G, and B regions (i.e., the HSI transformation assumes an infinitely narrow color response);
- The HIS model only includes the values of the R, G, and B bands in the transformation, while the imagery may include more bands of color information, e.g., the QuickBird images also include Near IR information.

As shown in Figure 1 and Figure 2, the multispectral coverage of the red, green, and blue bands does not cover the full spectrum of the panchromatic band. In this case we expect a simple component substitution technique to suffer from some color distortion. To minimize this color distortion, some authors (Strait 2008, Zhang 2004) model the panchromatic intensity from the multispectral bands and employ an equation as follows:

$$Pan_{\mathrm{model}}[k] = \sum_{i=1}^{N} C[i]MS[i][k] \qquad \textbf{Equation 2}$$

where "k" indicates a specific pixel in the image, MS[i][k] indicates the multi-spectral pixel for band "i" and location "k" in the image (typically derived from the upsampled image, at the same native resolution image as the panchromatic band), Pan_{model} is a "model" of the panchromatic band, and C is a vector of constants.

The constants "C" can be computed in a couple of different ways usually by purely statistical means. The problem with the technique is that the determination of these constants is often time consuming as it may require a lot of computation (as in Zhang 2004 in which the full pan-multispectral covariance matrix is required to be computed). They can also be determined by computing the exact spectral overlap of each multi-spectral band with the panchromatic band. In this case the constants must be computed separately for each sensor under consideration and this requires access to the detailed spectral response curves from the satellite provider, and such information may not be readily available.

In this paper we present a new pan-sharpening algorithm called Hyperspherical Color Sharpening (HCS). This algorithm handles any number of input bands and thus is an ideal candidate for sharpening WV-2 imagery. We first present the mathematics required for the forward and reverse transformations to and from the native color space to the hyperspherical color space. Next, we apply the hyperspherical transformation to pan-sharpening and detail the operation of the algorithm. We also present a new pan sharpening quality index that measures both the spectral quality and the spatial quality of the pan sharpened image, with respect to the original multispectral and panchromatic images. The quality index is found to correlate with visual observations that we make concerning the pan-sharpened imagery. Finally we run a detailed experiment on 10 different WV-2 images representing a variety of land cover types and quantitatively compare the performance of the HCS algorithm to the well known Principal Components Algorithm (PCA, Chavez 1991) and the Gramm-Schmidt algorithm (GS, Laben et. al.).

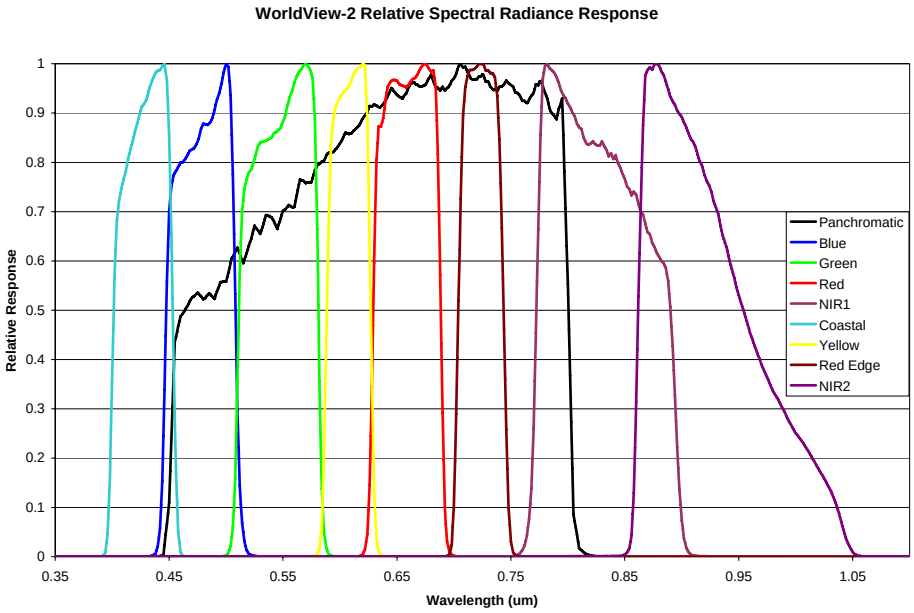

Figure 1. The relative spectral responses of the WV-2 satellite.

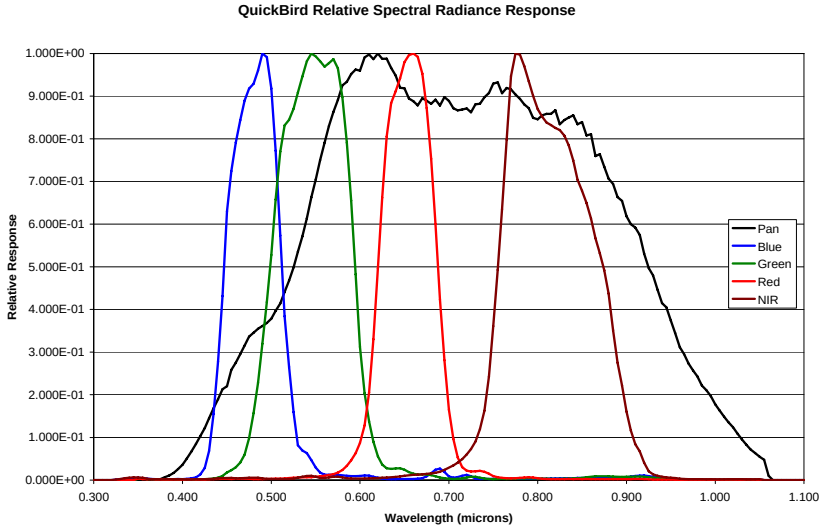

Figure 2. The relative spectral response of the QuickBird satellite.

HYPERSPHERICAL COLOR SPACE

The transformation between the native color space and the hyperspherical color space follows the standard definition of transformation between n-dimensional Cartesian space and n-dimensional hyperspherical space.

For an image with *N* input bands, one forms a single intensity component and *N-1* angles on the hypersphere. The general transformation into the HCS from an *N*-band color space is given by the following equations:

$$I = \sqrt{\chi_1^2 + \chi_2^2 + \ldots + \chi_n^2} \qquad \textbf{Equation 3}$$

$$\varphi_1 = \tan^{-1}\left(\frac{\sqrt{\chi_n^2 + \chi_{n-1}^2 + \cdots + \chi_2^2}}{\chi_1}\right) \qquad \textbf{Equation 4}$$

$$\varphi_{n-2} = \tan^{-1}\left(\frac{\sqrt{\chi_n^2 + \chi_{n-1}^2}}{\chi_{n-2}}\right) \qquad \textbf{Equation 5}$$

$$\varphi_{n-1} = \tan^{-1}\left(\frac{\chi_n}{\chi_{n-1}}\right) \qquad \textbf{Equation 6}$$

where χ_i is the i^{th} component of the native color space. The reverse transformation is:

$$\chi_1 = I\cos\varphi_1 \qquad \textbf{Equation 7}$$

$$\chi_2 = I\sin\varphi_1\cos\varphi_2 \qquad \textbf{Equation 8}$$

$$\chi_{n-1} = I\sin\varphi_1\sin\varphi_2\cdots\sin\varphi_{n-2}\cos\varphi_{n-1} \qquad \textbf{Equation 9}$$

$$\chi_n = I\sin\varphi_1\sin\varphi_2\cdots\sin\varphi_{n-2}\sin\varphi_{n-1} \qquad \textbf{Equation 10}$$

More specifically, for a common four-band image consisting of Blue, Green, Red, and Near IR (BGRN), the transformation is:

$$I = \sqrt{B^2 + G^2 + R^2 + N^2} \qquad \textbf{Equation 11}$$

$$\varphi_1 = \tan^{-1}\left(\frac{\sqrt{N^2 + R^2 + G^2}}{B}\right) \qquad \textbf{Equation 12}$$

$$\varphi_2 = \tan^{-1}\left(\frac{\sqrt{N^2 + R^2}}{G}\right) \qquad \textbf{Equation 13}$$

$$\varphi_3 = \tan^{-1}\left(\frac{N}{R}\right) \qquad \textbf{Equation 14}$$

Likewise, for the common four-band BGRN image, the reverse transformation is

$$B = I\cos\varphi_1 \qquad \textbf{Equation 15}$$

$$G = I\sin\varphi_1\cos\varphi_2 \qquad \textbf{Equation 16}$$

$$R = I\sin\varphi_1\sin\varphi_2\cos\varphi_3 \qquad \textbf{Equation 17}$$

$$N = I\sin\varphi_1\sin\varphi_2\sin\varphi_3 \qquad \textbf{Equation 18}$$

In the transformation to HCS, the angular (φ_n) variables define the color or hue while the radial (I) component

defines the intensity of the color. Once transformed into HCS, the intensity can be scaled without changing the color, essential for the HCS pan-sharpening algorithm.

The transformation to HCS can be made from *any* native color space (or pseudo color space in the case of pan-colorization). An example transformation is given below where RGB is transformed into HCS and plotted as a function of φ_1 and φ_2 at constant intensity.

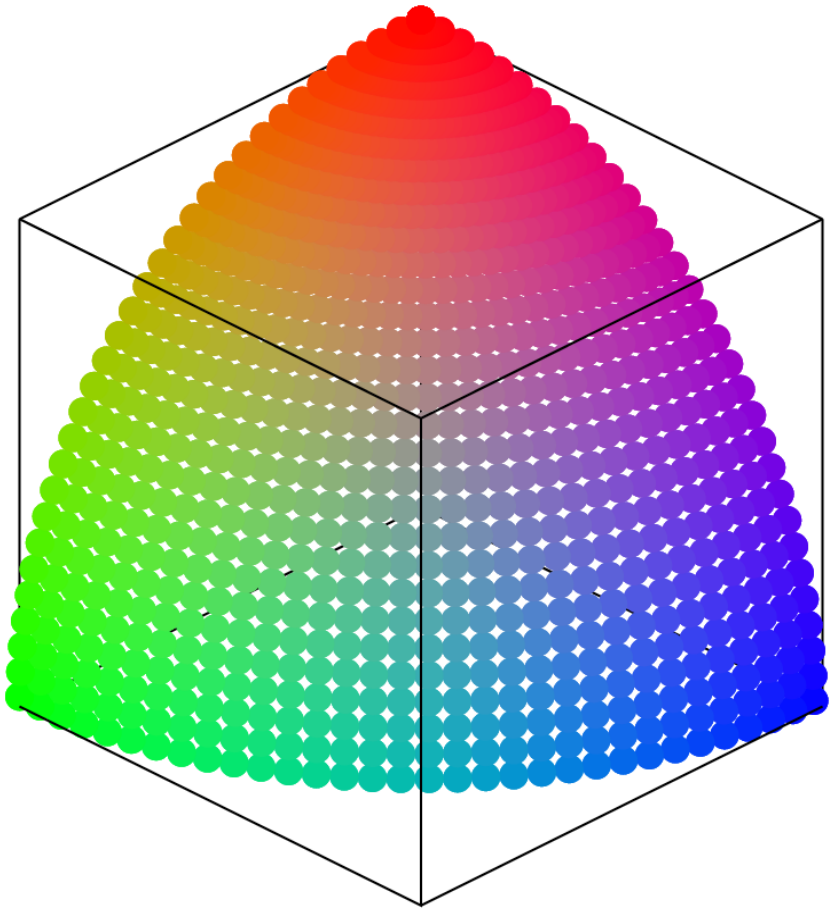

Fig 1. Transformation from RGB to HCS at constant intensity. This figure is a shell of constant radius (intensity) in the positive octant. As all color components are positive, the angular components of HCS span the space $[0, \pi/2]$. At $(\varphi_1,\varphi_2)=(0,0)$, the HCS represents pure red, as φ_1 is swept down to 90^o, the color changes along what would be the Red-Green axis in the RGB space, and sweeping φ_2 to 90^o is equivalent to movement along the Green-Blue axis in RGB space. Intensity is represented as the distance from the origin, which is constant in this figure. It is important to remember that the transformation into HCS is completely general and the final result depends on the native color space.

HYPERSPHERICAL PAN-SHARPENING

We describe two modes of operation of the HCS pan-sharpening algorithm. The first mode is called the *naïve* mode and simply replaces the multi-spectral intensity component with an intensity matched version of the pan band. Naïve mode has the advantage that it is simple to implement. Generally this provides a sharp image but some color distortion is noticeable in the resulting pan-sharpened image, as we are assuming that each multispectral band contributes equally to the panchromatic intensity.

The naïve mode proceeds as follows. We make a first pass through the data and compute the mean and standard deviation of both the square of the multispectral intensity and the mean and standard deviation of the square of the panchromatic intensity, given by:

$$I^2 = \sum_{i=1}^{N} \chi_i^2$$
$$P^2 = (Pan)^2 \qquad \textbf{Equation 19}$$

Let the mean and standard deviation of P^2 be denoted by μ_1 and σ_1, and let the mean and standard deviation of I^2 be denoted by μ_0 and σ_0. These quantities can be computed at a lower resolution to save time without adversely affecting the results. Next, we perform the forward transform from the native color space to the hyperspherical color space using equations 3-6.

Next, we intensity match the P^2 signal to the I^2 signal using the following equation:

$$P^2 = \frac{\sigma_0}{\sigma_1}\left(P^2 - \mu_1 + \sigma_1\right) + \mu_0 - \sigma_0 \qquad \textbf{Equation 20}$$

The sharpening step is performed by forming the adjusted intensity by taking the square root of the P^2 band as follows:

$$I_{adj} = \sqrt{P^2} \qquad \textbf{Equation 21}$$

The resulting I_{adj} is the pan-sharpened intensity. The sharpening algorithm proceeds by directly substituting the quantity I_{adj} for I in equations 7-10 in the reverse transformation from HCS color space back to the original color space.

The second mode is called the *smart* mode. We have found that this mode does an acceptable job of replicating the original multi-spectral colors. The reason for this is that this mode models the difference between the pan and multispectral intensity and accounts for this difference during the pan sharpening process while *naïve* mode does not.

Smart mode proceeds as follows. Prior to sharpening the image we form a smoothed version of the panchromatic band as follows:

$$Pan_{smooth} = SMOOTH(pan) \qquad \textbf{Equation 22}$$

where the *SMOOTH* operation is simply a sliding window convolution filter, performed with a 7x7 square window, in which the value of the middle output pixel is the mean of all pixels in the window. The dimensions of the window may be adjusted; however, we observe the fewest spatial artifacts[3] in the resulting pan-sharpened image when the size of the window is set to 7x7.

Next we compute the mean and standard deviation of both the square of Pan_{smooth} band (PS^2) and the square of the multispectral intensity (I^2), given by

$$I^2 = \sum_{i=1}^{N} \chi_i^2$$
$$PS^2 = \left(Pan_{smooth}\right)^2 \qquad \textbf{Equation 23}$$

Let the mean and standard deviation of PS^2 be denoted by μ_1 and σ_1, and let the mean and standard deviation of I^2 be denoted by μ_0 and σ_0. As in naïve mode, computation of these quantities requires a pass through the data, but can be computed at a lower resolution to save time without adversely affecting the results. Next, we perform the forward transform from the native color space to the hyperspherical color space using equations 3-6.

[3] The goal is to match the multi-spectral resolution as best as possible. Using smaller or larger window sizes can cause spatial artifacts like ghosting and blurring in the resulting products.

Next, we intensity match both the P^2 and the PS^2 signal to the I^2 signal using the following equations:

$$PS^2 = \frac{\sigma_0}{\sigma_1}\left(PS^2 - \mu_1 + \sigma_1\right) + \mu_0 - \sigma_0$$

$$P^2 = \frac{\sigma_0}{\sigma_1}\left(P^2 - \mu_1 + \sigma_1\right) + \mu_0 - \sigma_0 \qquad \textbf{Equation 24}$$

Next we form a quantity called the adjusted intensity as follows:

$$I_{adj} = \sqrt{\frac{P^2}{PS^2} I^2} \qquad \textbf{Equation 25}$$

The resulting I_{adj} is the pan-sharpened intensity. The sharpening algorithm proceeds by directly substituting the quantity I_{adj} for I in equations 7-10.

PAN-SHARPENING PERFORMANCE EVALUATION

An obvious question is how to evaluate the performance of a given pan-sharpening algorithm. A good pan-sharpening result will exhibit excellent spatial quality (i.e. recovery of edges) and also will maintain the colors of the original multispectral image. But how does one evaluate these quantitatively?

There exist many methods to assess both the spectral and spatial quality of the pan-sharpened image. Currently there is no consensus in the literature (Li 2000) on the best quality index for pan-sharpening. The reader is referred to Strait et. al. (2008) for a survey of many of the methods employed in the literature. One of these methods is the Wang-Bovic (Wang, Bovic 2002) quality index. Borel et. al. (2009) demonstrates utility of the Wang-Bovic quality index for evaluating pan-sharpening performance. The Wang-Bovic quality index for two images *f* and *g* is defined as

$$Q_{WB} = \frac{\sigma_{fg}}{\sigma_f \sigma_g} \frac{2\mu_f \mu_g}{\mu_f + \mu_g} \frac{2\sigma_f \sigma_g}{\left(\mu_f^2 + \mu_g^2\right)\left(\sigma_f + \sigma_g\right)} \qquad \textbf{Equation 26}$$

where the variances are represented as σ_f and σ_g and the means are represented as μ_f and μ_g. Following Wang-Bovic, the first term is the spatial cross correlation between *f* and *g*, the second term is a comparison of the means between *f* and *g*, and the third term is a comparison of the contrasts. The index goes between -1 and 1. When the image *f* is considered to be the original, unaltered image, and the image *g* is considered to be the altered image, then QWB is considered to measure the quality of *g* with respect to *f*.

In order to apply the Wang-Bovic quality index, one must have a reference image. This presents a problem for pan-sharpening since no reference image exists at the pan-sharpened resolution. Invariably one must downsample the pan-sharpened image to the original multispectral resolution, which allows direct computation of the quality index. The Q_{WB} can be computed at a certain scale, or block size. Following Borel we use a block size of approximately ¼ of the image.

The Wang-Bovic quality index can be computed for each band in the original multi-spectral image, producing a vector of values. We define the quantity Q_λ as follows

$$Q_\lambda = \left[Q_{WB}(MS_1, PS_1), Q_{WB}(MS_2, PS_2), \ldots, Q_{WB}(MS_N, PS_N)\right] \qquad \textbf{Equation 27}$$

where *MS* indicates the original multispectral band in the image, and *PS* indicates the pan-sharpened band (downsampled to the multispectral resolution), and *N* is the number of bands in the image.

However, we argue that the computation of QWB alone is unsatisfactory to fully evaluate pan-sharpening quality. Since the computation is carried out at the same spatial resolution as the multispectral image, the Q_{WB} index cannot evaluate the spatial quality of the image at the panchromatic resolution.

For evaluating the **spatial performance** of a pan-sharpening algorithm, we have found that simply computing the cross correlation of the original pan band with each band of the pan-sharpened image provides an effective measure of spatial quality. The cross correlation of two signals A and B is defined as:

$$CC(A,B) = \frac{\sum (A_i - \mu_A)(B_i - \mu_B)}{\sqrt{\sum (A_i - \mu_A)^2 \sum (B_i - \mu_B)^2}} \qquad \textbf{Equation 28}$$

where μ_A and μ_B are the means of signals *A* and *B*, and the summation runs over all elements of each signal. The CC metric goes from -1 to 1.

The cross correlation can be computed between the pan band and every band in the pan-sharpened image producing a vector of values. We define the quantity CC_λ as:

$$CC_\lambda = \left[CC(Pan, PS_1), CC(Pan, PS_2), ..., CC(Pan, PS_N) \right] \qquad \textbf{Equation 29}$$

where *Pan* indicates the panchromatic band, and *PS* indicates the pan-sharpened band, with the subscript indicating the band index, and *N* is the number of bands in the image.

In this work we propose a new quality metric for pan-sharpening. The quality metric has two elements, spectral quality and spatial quality. The spectral quality is the Wang-Bovic quality index and the spatial quality is simply the cross correlation. We define the quantity Q_{PS} as follows:

$$Q_{PS} = \left(\frac{1}{N} \sum_{\lambda=1}^{N} Q_\lambda \right) \times \left(\frac{1}{N} \sum_{\lambda=1}^{N} CC_\lambda \right) \qquad \textbf{Equation 30}$$

where Q_λ and CC_λ are defined above. The index ranges from -1 to 1. A good pan-sharpening quality index will provide a natural mechanism to evaluate and compare the performance of different pan-sharpening algorithms. As an example, we apply four different pan-sharpening algorithms to the same dataset and compute Q_{PS} for each algorithm and compare and contrast the results.

Table 1. Pan-sharpening quality computed for four different pan-sharpening algorithms for the same WV-2 input image.

Algorithm	Q_{red}	Q_{green}	Q_{blue}	CC_{red}	CC_{green}	CC_{blue}	Ave(Q_λ)	Ave(CC_λ)	Q_{PS}
PCA	0.891	0.878	0.898	0.847	0.859	0.816	0.889	0.841	**0.747**
GS	0.898	0.886	0.900	0.882	0.869	0.853	0.895	0.868	**0.777**
HIS	0.920	0.860	0.780	0.960	0.996	0.984	0.853	0.980	**0.836**
HCS Smart	0.929	0.904	0.878	0.929	0.946	0.909	0.904	0.928	**0.839**

The results are summarized in Table 1. The four algorithms compared are the Hue-Intensity-Saturation (HIS) algorithm, the Principal Components Analysis (PCA) algorithm, the Gramm-Schmidt (GS) algorithm, and the HCS smart algorithm. Analyzing the table we see that the algorithm's performance can be ranked quantitatively in terms of the Q_{PS} metric, and we can make several quantitative observations concerning each algorithm's performance. The PCA algorithm scores the lowest of the four, and is the least sharp of all the algorithms. The GS algorithm is sharper than PCA, and retains the spectral quality better than PCA, and thus scores higher than PCA. The spectral quality for the HIS algorithm is very poor, with the blue band being the worst (0.78), but the spatial quality is quite high (0.98). Thus the poor spectral performance is offset by the excellent spatial performance and the algorithm scores higher than both PCA and GS. The HCS algorithm scores high in both spectral and spatial performance and scores the highest out of all four algorithms.

Thus we conclude that spectrally speaking, HCS produces the best result, followed closely by GS and PCA, while HIS produces the worst result. Spatially speaking, HIS is the sharpest algorithm, followed by HCS, then GS, then PCA. Overall the HCS algorithm maintains the best balance between spectral and spatial quality of the 4 algorithms.

How do these quantitative observations correlate with quantitative observations that we may make about the imagery? Referring to Figure 3, we see that the HIS algorithm produces sharp imagery and visually speaking looks as sharp as the panchromatic image, but there is an overall blue color to the vegetation that looks very different from the original multispectral image. The PCA, GS, and HCS algorithms all exhibit much better color recovery than the HIS algorithm. The PCA algorithm exhibits some visible artifacts, notably some discoloration around the white building near the top right, and the overall result is blurrier than the original pan image. The GS algorithm has fewer artifacts than PCA, but still exhibits some discoloration around the white building near the top right. The overall result looks sharper than the PCA result, but is not as sharp as the panchromatic image. The HCS result exhibits no discoloration around the white building near the top right, and exhibits the fewest visible artifacts. The HCS result is sharp and looks nearly as sharp as the panchromatic image.

In summary, we conclude that the pan-sharpened quality index proposed here correlates with qualitative observations we may make concerning the imagery and is a useful measure of pan-sharpening performance.

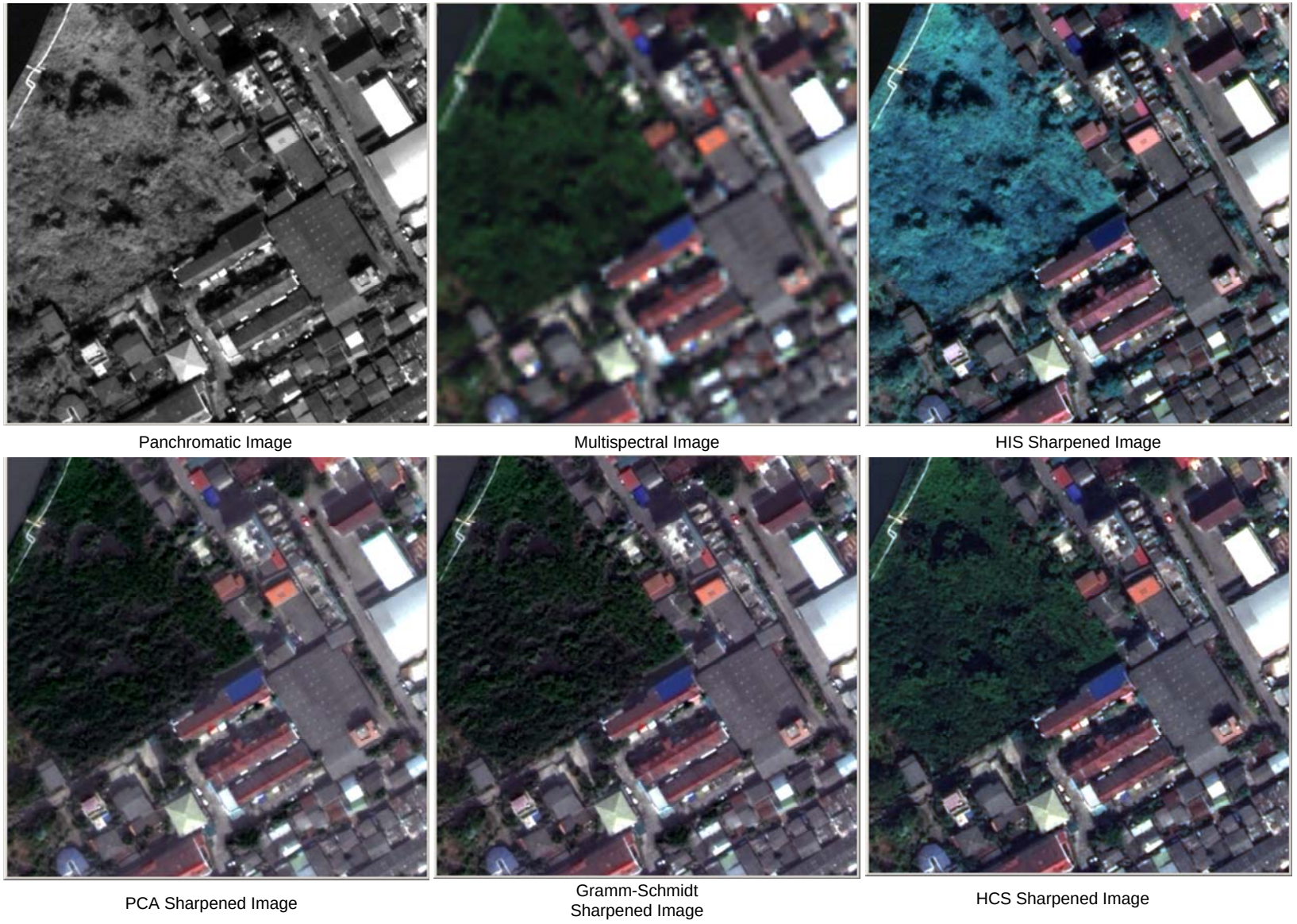

Figure 3. Comparison of performance between the HIS, PCA, GS, and HCS pan-sharpening algorithms for a WV-2 image.

EXPERIMENTAL RESULTS

We performed the following experiment to evaluate and compare the performance of the HCS smart algorithm against both the GS and PCA algorithms available in ENVI. We collected 10 scenes with the WV-2 satellite of a variety of different types of land cover, including Desert, Urban, Coastal, Forest, Rock, and Snow scenes. Each image measured 10,000 pixels by 10,000 lines. All the WV-2 imagery was ordered as Pan-MS1-MS2 bundle products. In this configuration the panchromatic and multispectral imagery are stored in separate image files. The WV-2 multispectral data, when ordered in this configuration, contains the bands ordered by increasing wavelength. The band order for a Pan-MS1-MS2 product is listed in Table 1.

Table 2. WV-2 band order for an 8 band bundle product.

Band Name	Band Index	Spectral Characteristics (nanometers)
Coastal	1	400-450
Blue	2	450-510
Green	3	510-580
Yellow	4	585-625
Red	5	630-690
Red Edge	6	705-745
Near IR 1	7	770-895
Near IR 2	8	860-1040

The data was prepared for pan-sharpening using the following process. The multi-spectral data was up-sampled to the same resolution as the panchromatic resolution (0.5m) using a bilinear resampling kernel. This kernel is used to suppress high frequency spatial artifacts in the up-sampled multispectral imagery that can cause visual artifacts in the pan-sharpened imagery. No explicit registration step was performed to align the panchromatic and multispectral data. The imagery was pan-sharpened using the HCS smart algorithm, the PCA algorithm, and the Gramm-Schmidt algorithm. The spatial and spectral quality indices were then computed in an automated fashion. The results of the experiment are presented in Table 3.

Table 3. WV-2 8 band pan-sharpening experimental results.

Land Cover Type	PCA			GS			HCS		
	Q_λ	Q_{CC}	Q_{PS}	Q_λ	Q_{CC}	Q_{PS}	Q_λ	Q_{CC}	Q_{PS}
Desert	-0.67	-0.85	0.56	0.94	0.84	0.80	0.83	0.94	0.78
Urban	0.94	0.78	0.73	0.94	0.79	0.74	0.82	0.90	0.74
Desert	0.96	0.98	0.94	0.96	0.98	0.95	0.96	0.98	0.94
Coastal	0.46	0.15	0.07	0.92	0.70	0.65	0.90	0.73	0.65
Snow	-0.77	-0.96	0.74	0.98	0.96	0.94	0.96	0.99	0.95
Forest	0.92	0.86	0.80	0.94	0.87	0.82	0.92	0.88	0.80
Rocks	0.85	0.90	0.76	0.85	0.90	0.76	0.60	0.97	0.59
Desert	0.76	0.98	0.74	0.75	0.98	0.74	1.00	0.98	0.97
Desert	-0.60	-0.87	0.52	0.91	0.88	0.81	0.83	0.93	0.77
Flood Basin	0.93	0.91	0.84	0.93	0.92	0.86	0.91	0.94	0.85
Average	0.38	0.29	**0.67**	0.91	0.88	**0.805**	**0.87**	**0.92**	**0.805**

Referring to Table 3, we note that the performance of the PCA algorithm is widely variable, often producing negative correlations when compared to the input multi-spectral or input panchromatic images (see the 1st, 5th, and 9th rows in the table). We assume this is due to a significant amount of energy being distributed into other bands for these scenes rather than just the 1st band of the principal components transform, a situation which is not modeled by the PCA sharpening algorithm. Note that the algorithm is not penalized by the quality index if both Q_λ and CC_λ are negative, as is the case for all the PCA examples that show negative spectral or spatial quality indices. The Gramm-Schmidt algorithm shows much better performance than the PCA algorithm over all cover types, and shows no evidence of negative correlations. This is due to the fact that the GS algorithm models the input bands in a better fashion than PCA

does, and is better equipped to handle histograms in which one multispectral component may overwhelm the other components. The HCS algorithm also performs well over all the input scenes (especially Desert, row 8). The overall quality index of HCS is tied with that of Gramm-Schmidt. We observe that GS appears to be stronger spectrally (0.91 versus 0.87) while the HCS algorithm appears to be stronger spatially (0.92 versus 0.88). Visual comparisons of the images confirm this observation regarding the sharpness (Figure 3).

It is interesting to note that sharpening all eight bands is not only possible, but also works quite well. Some examples of different band combinations displayed in RGB format are shown in Figure 4. This may be somewhat surprising to the casual reader who may expect that the sharpening would be naturally limited to only those multispectral bands which offer significant spectral overlap with the panchromatic band. The reality is that the HCS algorithm models the data statistically instead of employing a physical model involving the exact spectral band passes of the sensor in question. Thus the spectral overlap of the bands is not a strong determining factor in the quality of the pan-sharpened image.

CONCLUSIONS

In this work we have presented a new pan-sharpening algorithm called Hyperspherical Color Sharpening (HCS) and have detailed the implementation of this algorithm. In addition we have presented a new quantitative measure of pan-sharpening performance that measures both spatial and spectral quality of the resulting pan-sharpened image, and agrees very well with visual observations that we might make about the imagery. We have quantitatively evaluated the performance of the HCS, PCA, and GS algorithms on WV-2 imagery collected over a variety of cover types. The results indicate that the HCS algorithm is the strongest spatially of the three algorithms while maintaining a reasonable color balance.

ACKNOWLEDGEMENTS

The authors would like to thank Vic Leonard, Sr. Technical Fellow at DigitalGlobe for many engaging conversations and thoughtful ideas concerning pan-sharpening.

REFERENCES

Borel, C., Spencer, C., Ewald, K., Wamsley, C., 2009. Novel methods for panchromatic sharpening of multi/hyper-spectral image data, 7/22/2009, SPIE conference paper.

Chavez, P.S., Sides, S.C., Anderson, J.A., 1991. Comparison of three difference methods to merge multiresolution and multispectral data: Landsat TM and SPOT panchromatic, *PE&RS,* 57, (1991) 295-303.

Choi, M.J., Kim, H.C., Cho, N.I., Kim, H.O. An Improved Intensity-Hue-Saturation Method for IKONOS Image Fusion, *Internation Journal of Remote Sensing*, in pre-print.

Khan, M.M., Alparone, L., Chanussot, J. Pansharpening Quality Assessment Using Modulation Transfer Function Filters.

Laben et. al. Process for Enhancing the Spatail Resolution of Multisepctral Imagery using Pan-Sharpening, US Patent 6,011,875.

Li, J., 2000. Spatial quality evaluation of fusion of different resolution images, *ISPRS Int. Arch. Photogramm. Remote Sens*., vol. 33, no. B2-2, pp-339-346.

Nikolakopoulos, K.G., 2008. Comparison of Nine Fusion Techniques for Very High Resolution Data, *PE&RS*, May 2008.

Strait, M., Rahmani, S., Markurjev, D., Wittman, T., Aug 2008. Evaluation of Pan-Sharpening Methods, Technical Report, UCLA Department of Mathematics.

Tu, T.M., Su, S.C., Shyu, H.C., Huang, P.S., 2001. A new look at HIS-like image fusion methods, *Information Fusion 2*, (2001), 177-186.

Tu, T.M., Huang, P.S., Hung, C.L., Chang, C.P., 2004. A Fast Intensity-Hue-Saturation Fusion Technique With spectral Adjustment for IKONOS Imagery, *IEEE Geoscience and Remote Sensing Letters*, Vol 1, No 4, October 2004.

Wang, Z., Bovic, A., 2002. A Universal Image Quality Index, *IEEE Signal Processing Letters*, Vol 9, No 3, March

2002.
Zhang, Y., 2002. A new automatic approach for effectively fusing Landsat 7 as well as Ikonos images, Proceedings of IEEE/IGARSS'02, Toronto, Canada, 4:2429-2431.
Zhang, Y., 2004. Understanding Image Fusion, *Photogrammetric Engineering and Remote Sensing*, 70(6):657-661, 2004.

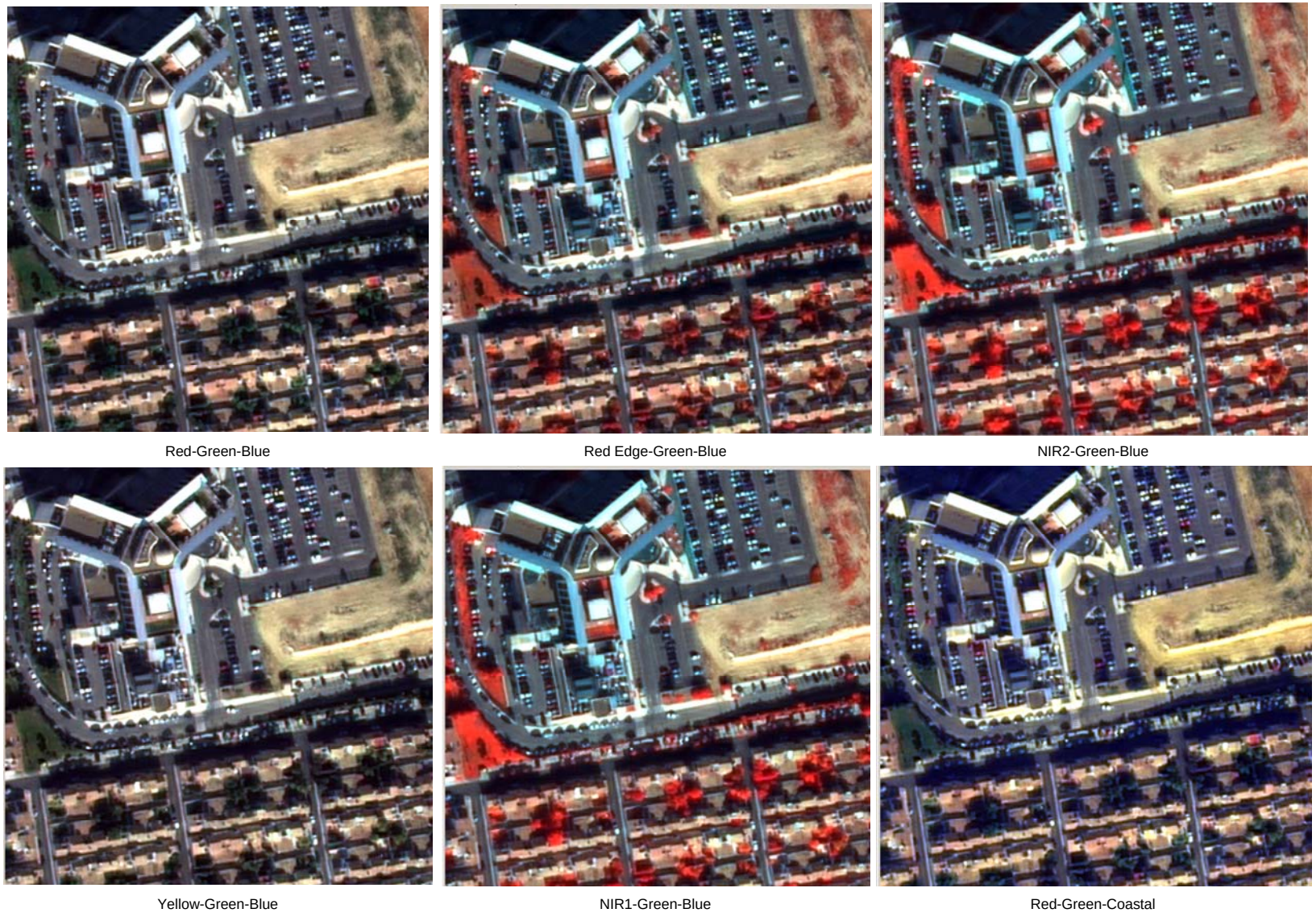

Figure 4: Different Pan-Sharpening band combinations, sharpened with the HCS algorithm.